

# Core-Collapse Simulations of Very Massive Stars: Gravitational Collapse, Black-hole Formation, and Beyond

Ninoy Rahman,<sup>a,\*</sup> H.-T. Janka,<sup>b</sup> G. Stockinger<sup>c</sup> and S. E. Woosley<sup>d</sup>

<sup>a</sup>*GSI Helmholtzzentrum für Schwerionenforschung,  
Planckstr. 1, 64291 Darmstadt, Germany*

<sup>b,c</sup>*Max Planck Institute for Astrophysics,  
Karl-Schwarzschild-Str. 1, Postfach 1317, D-85741 Garching, Germany*

<sup>c</sup>*Physik-Department, Technische Universität München,  
James-Franck-Str. 1, D-85748 Garching, Germany*

<sup>d</sup>*Department of Astronomy and Astrophysics, University of California,  
Santa Cruz, CA 95064, USA*

*E-mail:* [n.rahman@gsi.de](mailto:n.rahman@gsi.de)

We study the final collapse of rotating and non-rotating very massive star progenitors with zero-age-main-sequence masses of 60, 80, and 115  $M_{\odot}$  by 2D hydrodynamics simulations. The general relativistic radiation hydrodynamics code NADA-FLD allows us to follow the evolution beyond the moment when the newly born neutron star (NS) collapses to a black hole (BH), which happens within 350–580 ms after bounce in all cases. In all cases except the rapidly rotating 60  $M_{\odot}$  model, neutrino heating leads to shock revival. In the rapidly rotating 60  $M_{\odot}$  model, centrifugal effects support higher NS mass but reduce the radiated neutrino luminosities and mean energies, and the value of neutrino-heating rate is smaller by roughly a factor of two compared to its non-rotating counterpart. After BH formation, the neutrino luminosities drop steeply but continue on a 1–2 orders of magnitude lower level for several 100 ms because of aspherical accretion of neutrino and shock-heated matter. In all shock-reviving models BH accretion swallows the entire neutrino-heated matter and the explosion energies decrease from maxima to zero within a few seconds latest. Nevertheless, the shock or a sonic pulse moves outward and may trigger mass loss, which we estimate by long-time simulations with the PROMETHEUS code.

*FAIRness 2022,  
23–27 May, 2022  
Mediterranean Village, 60100 Paralia Katerinis, Greece*

---

\*Speaker

## 1. Introduction

In this study, we conduct core-collapse supernova (CCSN) simulations of very massive stars (VMSs) with pre-SN helium core masses between  $\sim 30 M_{\odot}$ – $65 M_{\odot}$ , corresponding to zero-age-main-sequence (ZAMS) masses roughly between  $70 M_{\odot}$ – $140 M_{\odot}$ . After core-carbon burning, a very massive star can experience pulsational pair-instability supernovae (PPISNe) when its pre-SN helium core mass is below  $\sim 65 M_{\odot}$ . On the other hand, the star can be completely destroyed in a single violent pulse called pair-instability supernova (PISN) if the helium core mass is above  $\sim 65 M_{\odot}$ . The PPISNe and PISN can occur in stellar cores with temperatures greater than  $\sim 7 \times 10^8$  K. Such a high temperature enables the onset of electron-positron pair production. This pair production converts the thermal energies of photons into rest mass energies of electron-positron pairs and reduces the structural adiabatic index below the critical limit of  $4/3$  for stability. Such a phenomenon is called “pair-instability” [3, 9, 17]. Due to this softening of the equation of state (EOS), the stellar core contracts and ignites nuclear burning of oxygen and/or silicon leading to the rebound of the core. In PISN, the whole star disrupts by a giant nuclear flash. Instead, in the case of PPISNe, the core undergoes consecutive implosions and expansions. These pulsations cause stellar mass shedding and the star can lose its hydrogen envelope and sometimes the outer layers of its helium shell as well (for further details regarding the stellar evolution of VMS progenitors studied here and their astrophysical implications, see, e.g., Woosley 19, Woosley & Heger 20). The gravitational collapse that follows the PPISNe phase can form rapidly spinning black holes (BHs) or strongly magnetized neutron stars (NSs) and possibly creates collimated, jet-like outflows [19]. Moreover, gravitational-wave (GW) signals radiated by the inspiral and merger of binary BHs with large masses of more than  $30 M_{\odot}$  have been detected by the LIGO and Virgo collaboration [1, 2] and the core-collapse of VMS can produce black holes with similar masses.

The core-collapse simulations of the VMSs are conducted using the general-relativistic hydrodynamics and transport code NADA-FLD [14, 15] in two dimensions employing the Steiner, Fischer, and Hempel (SHFo) EOS [11, 18]. The long-time simulations of the shock or sonic pulse propagation through the stellar material is conducted with the PROMETHEUS code [10].

## 2. Results

In Table 1, we list our model names, ZAMS masses of VMS progenitors, baryonic masses of the pre-collapse stars, iron core masses at the onset of stellar core collapse, compactness parameters of inner core of  $2.5 M_{\odot}$ , total angular momenta of progenitors, Kerr parameters of the progenitor stars. Furthermore, we show the post-bounce times at the onset of shock revival and the post-bounce times at the moment of BH formation. We notice that all models have massive iron-cores and large compactness parameters which result in high mass accretion rates onto the newly born proto-neutron stars (PNSs). These high mass accretion rates generate large luminosities for the electron type neutrino species and lead to substantial net heating rates by neutrinos in the gain layer. As a consequence, Models C60C-NR, R80Ar-NR, R80Ar, and C115 experience shock revival around 200 ms after bounce as shown by top-left panel of Fig. 1.

In Fig. 1, the post-bounce time evolution of the angle-averaged shock radius (top-left panel), PNS baryonic mass (top-right panel), central baryonic density (bottom-left panel), and electron

**Table 1:** Progenitor properties and characteristic properties of the simulated models.

Model	$M_{\text{ZAMS}}$ [ $M_{\odot}$ ]	$M_{\text{prog}}$ [ $M_{\odot}$ ]	$M_{\text{Fe}}$ [ $M_{\odot}$ ]	compactness	$J_{\text{prog}}$ [ $10^{50}$ erg s]	$a_{\text{prog}}$	$t_{\text{sh-rev}}$ [s]	$t_{\text{BH}}$ [s]
C60C-NR	60	41.54	2.37	0.77			0.250	0.580
C60C	60	41.54	2.37	0.77	105	0.55		0.510
R80Ar-NR	80	47.64	2.72	0.84			0.246	0.350
R80Ar	80	47.64	2.72	0.84	14	0.07	0.237	0.350
C115	115	45.50	2.46	0.89			0.222	0.400

*Notes:*  $M_{\text{ZAMS}}$  is the ZAMS mass of the progenitor,  $M_{\text{prog}}$  is the gravitationally bound baryonic mass of the pre-collapse star,  $M_{\text{Fe}}$  is the iron core mass,  $J_{\text{prog}}$  is the total angular momentum of the gravitationally bound progenitor mass,  $a_{\text{prog}}$  is the Kerr parameter of the gravitationally bound progenitor, all given at the onset of stellar Fe-core collapse. All models have zero-age-main-sequence (ZAMS) metallicity of 10%  $Z_{\odot}$ . Furthermore,  $t_{\text{sh-exp}}$  denotes the post-bounce time at the onset of shock revival (i.e., the post-bounce time when the angle-averaged shock radius reaches a value of 400 km),  $t_{\text{BH}}$  is the post-bounce time when a BH begins to form. The time of BH formation is defined by the moment when the apparent horizon finder first detects the appearance of an event horizon.

neutrino luminosity (bottom-right panel) at a radial distance of 500 km are shown for all of our models. Due to ongoing mass accretion, the PNS masses grow in all models. When the PNS mass crosses the maximum mass supported by the finite temperature nuclear EOS and the centrifugal force of a rotating model, the PNS collapses to a BH. Our Models C60C-NR (brown line), C60C (violet line), R80Ar-NR (orange line), R80Ar (green line), and C115 (blue line) form BHs around 580, 510, 350, 350, and 400 ms after core bounce, respectively, and the BH formation times are marked by the steep rises in central baryonic densities. At the time of BH formation, the neutrino luminosities drop by 1–2 orders of magnitude, however, the RMS energies of the radiated neutrinos after the BH formation are considerably higher than that of the PNS cooling phase, namely up to more than 25 MeV for electron neutrinos, more than 30 MeV for electron anti-neutrinos, and even more than 50 MeV for heavy-lepton neutrinos.

After the BH formation, the outflow of matter from the central compact object ceases. The high-entropy plumes produced by the neutrino heating before the BH formation have lower density and higher temperature compared to their surrounding matter and therefore their outer parts continue to expand for a transient time after BH formation. Due to the buoyancy forces, these high-entropy plumes rise radially outward and expand in all directions. These expanding plumes transfer energy and momentum to the surrounding material and the shock by mechanical work [4, 5]. Eventually, the bubbles containing the originally neutrino-heated gas fall back to the BH, but the shock continues to expand in our models. However, if enough energy is gained by the shock before the fallback of high-entropy plumes, the shock can reach the stellar surface.

To study the shock propagation through the stellar matter, we mapped our NADA-FLD models with shock revival to the PROMETHEUS code. In the PROMETHEUS simulations, the innermost 400 km are excised to increase the integration times step and are replaced by a point mass and an open inner

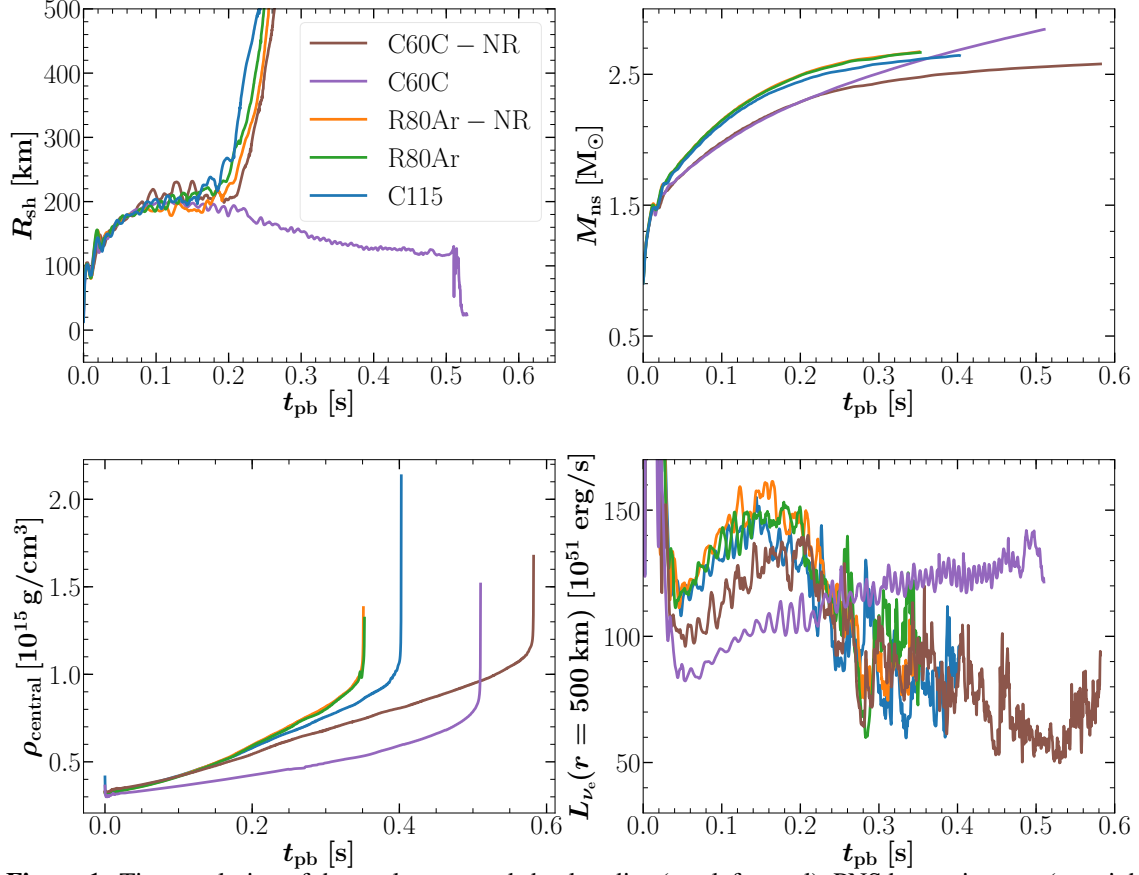


**Figure 1:** Time evolution of the angle-averaged shock radius (top-left panel), PNS baryonic mass (top-right panel), central baryonic density (bottom-left panel), and electron neutrino luminosity evaluated at  $r = 500$  km for all of our models. Models C60C-NR (brown line), C60C (violet line), R80Ar-NR (orange line), R80Ar (green line), and C115 (blue line) experience shock expansion around 200 ms after bounce and form BHs at 580, 510, 350, 350, and 400 ms after core bounce, respectively.

**Table 2:** Upper bound of ejecta mass.

Model	Mode	Upper bound of ejecta mass [ $M_{\odot}$ ]
C60C-NR	shock	0.14
R80Ar-NR	shock $\rightarrow$ sonic pulse	1.1
R80Ar	shock $\rightarrow$ sonic pulse	3.5
C115	shock $\rightarrow$ sonic pulse	0.07

boundary condition that allows the inflowing matter to cross the inner boundary of computational domain. At the time of the mapping, the radial infall velocities at the inner boundary are supersonic; therefore, hydrodynamical quantities outside the inner boundary can not be influenced by the properties of the flow through the inner boundary.

In Fig. 2, we show the mass-shell plot for Model C60C-NR as an example of models with shock revival. The shock radius and the stellar radius are marked by brown and green lines, respectively, and the quantity  $r^3\rho(r)$  is colour-coded in Fig. 2. In the region with positive radial

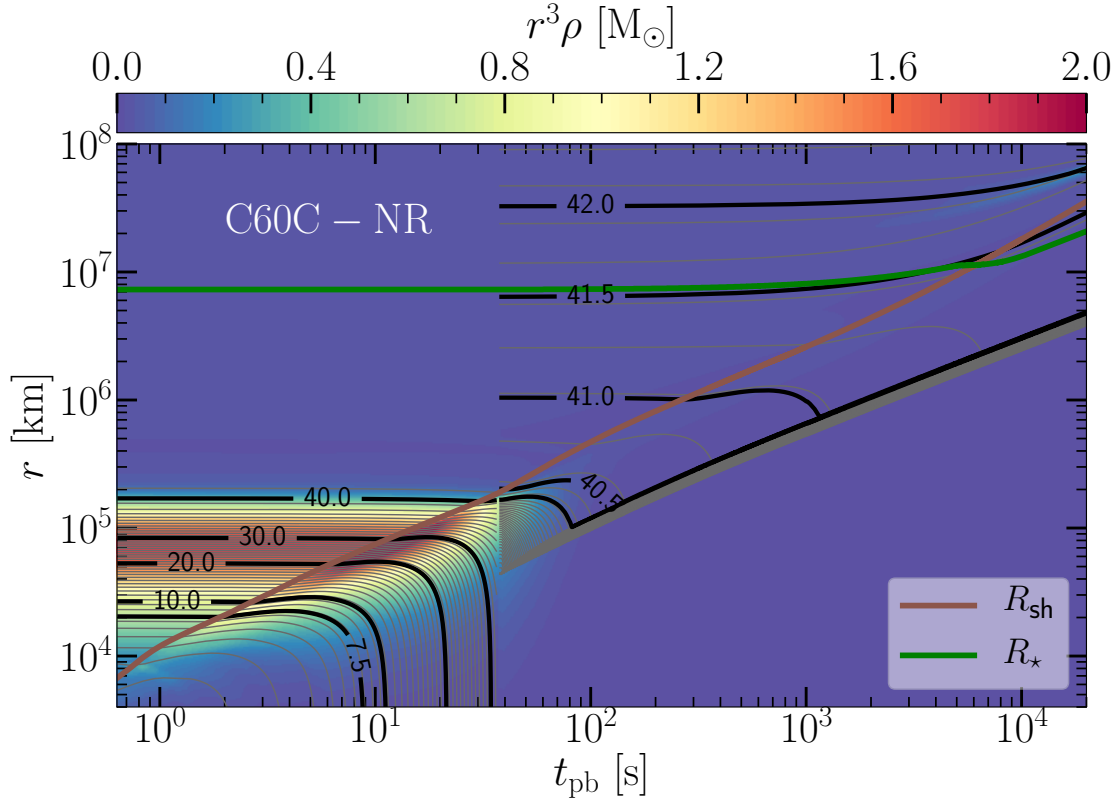


**Figure 2:** Mass-shell plots for Model C60C-NR. The quantity  $r^3\rho(r)$ , where  $\rho$  is the baryonic mass density, is color-coded. In addition, the shock radius,  $R_{\text{sh}}$  (brown line), and the radius of the star,  $R_{\star}$  (green line), are marked. Several of the mass shells are highlighted by black lines with mass labels. The interface between the Si-O layer and the O layer is at a mass coordinate of  $7.54 M_{\odot}$ .

gradient of  $r^3\rho(r)$ , an expanding shock with constant energy experiences deceleration. Therefore, when moving through the Si- and O-shells, the outgoing shocks in all our models with shock revival slow down as they have to move against the steep slope of  $r^3\rho(r)$ . Solely in Model C60C-NR, the shock survives this deceleration and in all other models, the shocks are converted to sonic pulses. When these shock and sonic pulses reach stellar surface, masses are ejected from stellar surfaces (for discussion regarding mass ejection by the sonic pulse, see e.g., Coughlin et al. 6, 7, 8, Linial et al. 12, Matzner & Ro 13). In Table 2, we show the upper bounds of ejecta mass for models with shock revival.

### 3. Summary

We study the core-collapse simulations of very massive stars and observe the formation of BHs with masses above  $40M_{\odot}$ . The general-relativistic hydrodynamics and transport code NADA-FLD allows us, for the first time, to predict neutrino signals beyond BH formation. Moreover, we provide estimates for mass ejected from the stellar surface due to the heating by the shock and the sonic pulse. Further details regarding our models are discussed in Rahman et al. [16].

Authors acknowledge funding by the European Research Council through Grant ERC-AdG No. 341157-COCO2CASA and by the Deutsche Forschungsgemeinschaft (DFG, German Research

Foundation) through Sonderforschungsbereich (Collaborative Research Centre) SFB-1258 “Neutrinos and Dark Matter in Astro- and Particle Physics (NDM)” and under Germany’s Excellence Strategy through Cluster of Excellence ORIGINS (EXC-2094)—390783311 and by the European Research Council (ERC) under the European Union’s Horizon 2020 research and innovation programme (ERC Advanced Grant KILONOVA No. 885281).

## References

- [1] Abbott B. P., et al., 2016, *Phys. Rev. Lett.*, 116, 061102
- [2] Abbott B. P., et al., 2019, *Astrophys. J. Lett.*, 882, L24
- [3] Barkat Z., Rakavy G., Sack N., 1967, *Phys. Rev. Lett.*, 18, 379
- [4] Chan C., Müller B., Heger A., Pakmor R., Springel V., 2018, *Astrophys. J. Lett.*, 852, L19
- [5] Chan C., Müller B., Heger A., 2020, *Mon. Not. R. Astron. Soc.*, 495, 3751
- [6] Coughlin E. R., Quataert E., Fernández R., Kasen D., 2018a, *Mon. Not. R. Astron. Soc.*, 477, 1225
- [7] Coughlin E. R., Quataert E., Ro S., 2018b, *Astrophys. J.*, 863, 158
- [8] Coughlin E. R., Ro S., Quataert E., 2019, *Astrophys. J.*, 874, 58
- [9] Fowler W. A., Hoyle F., 1964, *Astrophys. J. Suppl.*, 9, 201
- [10] Fryxell B., Mueller E., Arnett D., 1991, *Astrophys. J.*, 367, 619
- [11] Hempel M., Fischer T., Schaffner-Bielich J., Liebendörfer M., 2012, *Astrophys. J.*, 748, 70
- [12] Linial I., Fuller J., Sari R., 2021, *Mon. Not. R. Astron. Soc.*, 501, 4266
- [13] Matzner C. D., Ro S., 2021, *Astrophys. J.*, 908, 23
- [14] Montero P. J., Baumgarte T. W., Müller E., 2014, *Phys. Rev. D*, 89, 084043
- [15] Rahman N., Just O., Janka H. T., 2019, *Mon. Not. R. Astron. Soc.*, 490, 3545
- [16] Rahman N., Janka H. T., Stockinger G., Woosley S. E., 2022, *Mon. Not. R. Astron. Soc.*, 512, 4503
- [17] Rakavy G., Shaviv G., 1967, *Astrophys. J.*, 148, 803
- [18] Steiner A. W., Hempel M., Fischer T., 2013, *Astrophys. J.*, 774, 17
- [19] Woosley S. E., 2017, *Astrophys. J.*, 836, 244
- [20] Woosley S. E., Heger A., 2015, in Vink J. S., ed., *Astrophysics and Space Science Library* Vol. 412, *Very Massive Stars in the Local Universe*. Springer International Publishing, Switzerland, p. 199 ([arXiv:1406.5657](https://arxiv.org/abs/1406.5657)), [doi:10.1007/978-3-319-09596-7\\_7](https://doi.org/10.1007/978-3-319-09596-7_7)